Letter

Long-range order and quantum criticality in a dissipative spin chain

Matthew W. Butcher,[1] J. H. Pixley,[2,3,4] and Andriy H. Nevidomskyy[1]

[1]Department of Physics & Astronomy, Rice University, Houston, Texas 77005, USA
[2]Department of Physics and Astronomy, Center for Materials Theory, Rutgers University, Piscataway, New Jersey 08854, USA
[3]Center for Computational Quantum Physics, Flatiron Institute, 162 5th Avenue, New York, New York 10010, USA
[4]Physics Department, Princeton University, Princeton, New Jersey 08544, USA

(Received 12 July 2021; revised 28 April 2022; accepted 2 May 2022; published 16 May 2022)

The environmental interaction is a fundamental consideration in any controlled quantum system. While an interaction with a dissipative bath can lead to decoherence, it can also provide desirable emergent effects including induced spin-spin correlations. In this Letter, we show that under quite general conditions, a dissipative bosonic bath can induce a long-range ordered phase, without the inclusion of any additional direct spin-spin couplings. Through a quantum-to-classical mapping and classical Monte Carlo simulation, we investigate the $T = 0$ quantum phase transition of an Ising chain embedded in a bosonic bath with Ohmic dissipation. We show that the quantum critical point is continuous, Lorentz invariant with a dynamical critical exponent $z = 1.07(9)$, has a correlation length exponent $\nu = 0.80(5)$, and anomalous exponent $\eta = 1.02(6)$, thus the universality class is distinct from the previously studied limiting cases. The implications of our results on experiments in ultracold atomic mixtures and qubit chains in dissipative environments are discussed.

DOI: 10.1103/PhysRevB.105.L180407

Decoherence of a quantum two-level system, due to its coupling to the environment, is a key issue in the experimental attempts to improve the stability of qubits for scalable quantum computation [1–6]. Originating with studies of the spin-boson model [7–12], the nature of decoherence in open quantum systems with bosonic dissipation has been the subject of many important experimental endeavors including ultracold atomic gases and ions [13–16]. When multiple qubits are coupled to the same bath, the dissipation can also induce interactions between distant qubits. This effect is reminiscent of the Ruderman-Kittel-Kasuya-Yosida (RKKY) interaction induced by Friedel oscillations in a Fermi gas [17–19], although the microscopic mechanism in the presence of a bosonic bath is clearly different. These boson-induced interactions can allow coherent quantum states to form in a variety of different systems as demonstrated in trapped ions [20], superconducting qubits in a microwave cavity [21,22], and ultracold Bose-Fermi mixtures [23–25].

A direct solution of dissipation-induced interactions in qubit arrays that includes both their retarded dynamics and long-range nature has remained out of reach. Instead, theoretical progress has focused on more simplified settings that either ignore the intersite dissipation-induced interactions or leave out the dynamical fluctuations of the bosonic medium. It has not been possible to assess the accuracy of such approximate descriptions as the full solution to the problem has been lacking. A model in which intersite interactions play a dominant role is a one-dimensional (1D) spin chain immersed in a bosonic bath. This system, shown in Fig. 1(a), can be realized using either a Bose-Fermi or a Bose-Bose mixture, by placing one atomic species into a deep optical lattice that is embedded in a Bose-Einstein condensate (BEC) [26]. When the coherence length of the BEC (also known as the healing length) is short, each spin is effectively coupled to its own independent bath. This approximation describes arrays of Josephson qubits leading to locally critical floating phases [27,28], as well as novel universality classes [29,30] when the intersite interactions are time averaged and restricted to nearest neighbors. In the opposite limit of a very long healing length, the bath couples to the total value of spin $S^z = \sum_i s_i^z$, resulting in effectively infinite-range bath-induced interactions and a (1D) Berezinskii-Kosterlitz-Thouless (BKT) transition [31–34].

In the general case, when the full spatial dependence of the bath interactions must be considered, interesting phenomena such as entanglement [35–37], and coherent dynamics [38–43] emerge. Novel effects are also seen in the multiple-spin case of the closely related Kondo systems, for example, leading to enhanced pairing [44] and gapless dissipative phases [26,29,45]. Clearly, the spatial variation of the bath-induced interactions produces nontrivial correlations between coupled spins. However, to elucidate their effect on ordering and criticality in a spin chain, it is essential to go to the thermodynamic limit, which has proven to be a very challenging problem. As we will show, the full solution to this problem yields qualitatively different results than the solutions to the approximate descriptions possess, demonstrating the importance and necessity of such a nonperturbative result.

In this Letter, we apply a quantum-to-classical mapping that transforms this 1D quantum problem into a frustrated long-range interacting Ising model in two dimensions, which we simulate using classical Monte Carlo. Our results demonstrate that a chain of free qubits develops long-range ferromagnetic (FM) order at finite temperature for a

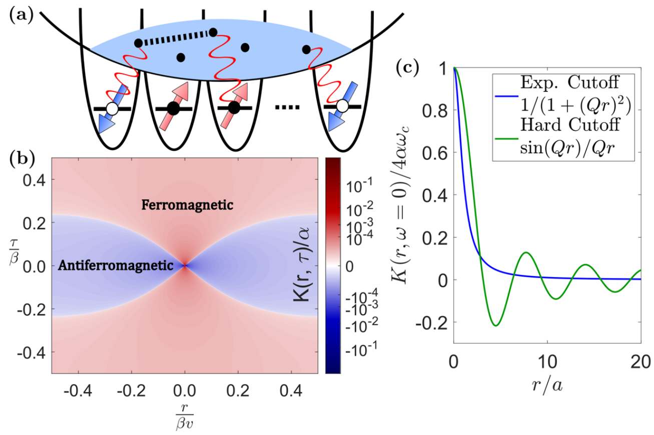

FIG. 1. (a) Local confining potentials trap particles in a two-state superposition, which maps to a chain of Ising pseudospins interacting with bath bosons. (b) Bath-induced interactions $K(r,\tau)$ given by Eq. (5) in the limit $\omega_c \to \infty$ ($\lambda \to 0$), with the color indicating the parity of the interaction. (c) Bosonic RKKY interactions for the cases of exponential and hard cutoffs, Eqs. (6) and (7), obtained by taking the static ($\omega = 0$) limit of $K(r,\tau)$, here with $Q = 1$

sufficiently strong coupling to the bath. We further show that a zero-temperature second-order quantum critical point (QCP) with emergent Lorentz symmetry separates a quantum paramagnet (QPM) from the FM phase. The critical exponents of this transition are distinct from previously studied models with direct spin-spin interactions and related dissipative spin models [29–32,46]. We emphasize that the long-range order arises purely from the spin-spin interactions induced by the dissipative bath, and that the universality class of the QCP is fundamentally determined by the long-range character of the bath-induced interactions. This finding provides proof of the existence of the bosonic analog of the RKKY effect and the possibility of boson-induced long-range order.

Bosonic RKKY effect. The shared bath results in the long-range temporal (retarded) and spatial interaction between the spins, which we refer to as the bosonic RKKY effect by analogy to the RKKY interaction between spins mediated by a Fermi gas. The analog of the $2k_F$ wave vector familiar from the fermionic RKKY effect is instead played by the ultraviolet (UV) scale that determines the truncation of the bath density of states, as shown below.

The model we consider is realized by a chain of spin-$\frac{1}{2}$ local moments (i.e., qubits) embedded in a shared bath of free bosons. The Hamiltonian, which we term the dissipative transverse field Ising model (DTFIM), is

$$H = -\Delta \sum_i \hat{\sigma}_i^x + \sum_k \omega_k \hat{b}_k^\dagger \hat{b}k + \sum_{i,k} \hat{\sigma}_i^z e^{ikr_i} g_k \hat{b}_k^\dagger + \text{H.c.} \quad (1)$$

Here, Δ is an applied transverse magnetic field, ω_k is the dispersion of bath modes, and g_k is the strength of the coupling between local moments and the bath bosons [26,29]. In the cold-atom implementation, for example, Δ originates from Raman laser-induced transitions, while g_k is proportional to the scattering length of the atomic species [26]. The Pauli matrices $\hat{\sigma}_i^x$ and $\hat{\sigma}_i^z$ act on the qubit at position r_i, while $\hat{b}_k^\dagger$ and $\hat{b}_k$ create and annihilate, respectively, the bath bosons with momentum k. We stress that in the limit of $g_k = 0$ the local moments are only coupled to the transverse field, which ensures that any induced long-range order is solely due to the dissipative bosonic bath. The bath bosons (phonons, in the case of a BEC bath [26]) are assumed to be in the acoustic regime, with linear dispersion $\omega_k = v|k|$, where v is the sound velocity of the condensate.

By integrating out the bosons and performing a quantum-to-classical mapping [47] (see Supplemental Material [48]), we arrive at the partition function of a 1 + 1-dimensional (1 + 1D) classical Ising model [49],

$$Z = Z_0 \sum_{\{s(r,\tau)\}} e^{-S_c},$$

$$S_c = -\Gamma \sum_{i,n} s(i,n)s(i,n+1)$$

$$-\tau_0^2 \sum_{i,j} \sum_{m,n} K(r_i - r_j, \tau_m - \tau_n) s(i,m)s(j,n). \quad (2)$$

The classical Ising variables $s(j,n)$ correspond to the eigenvalues of $\hat{\sigma}_j^z$ at position $r_j \equiv ja$ along the chain and imaginary time $\tau_n \equiv n\tau_0$. Here, $Z_0 = \prod_k (1 - e^{-\beta\omega_k})^{-1}$ is the free boson partition function. The nearest-neighbor imaginary-time coupling $\Gamma = -\frac{1}{2}\ln[\tanh(\Delta\tau_0)]$ arises from the quantum-to-classical mapping [47,48]. In the absence of dissipation ($g_k = 0$), this term sets the corresponding imaginary-time correlation length $\xi_\tau \sim \Delta^{-1}$. This local coupling simply renormalizes the finite ξ_τ when $g_k \neq 0$ and does not change the universal properties, so we can set $\Delta = 1$ without loss of generality [29]. The spatial and imaginary-time dimensions of the system have lengths L and $\beta = N\tau_0$, respectively, with lattice constant $a = 1$.

Coupling to the bath is captured by the spectral density [9,10] $J(\omega) = \pi \sum_k |g_k|^2 \delta(\omega - \omega_k)$. For the case of acoustic phonons in the BEC, the couplings g_k in Eq. (1) scale as $g_k \sim k^{1/2}$ [26], and the resulting spectral density is Ohmic, i.e., linear in frequency,

$$J(\omega) = 2\pi\alpha\omega f(\omega/\omega_c). \quad (3)$$

Here, α is a dimensionless parameter characterizing the dissipation strength of the bath. The cutoff function $f(\omega/\omega_c)$ depends on the physical setting and must decay to zero as ω exceeds the cutoff frequency ω_c [10]. This cutoff function is often taken to be smooth or abrupt,

$$f(\omega/\omega_c) = e^{-\omega/\omega_c}, \quad \text{“exponential” cutoff,}$$

$$f(\omega/\omega_c) = \Theta(1 - \omega/\omega_c), \quad \text{“hard” cutoff,} \quad (4)$$

where Θ is the Heaviside step function.

The bath-induced interactions $K(r,\tau)$ take the form

$$K(r,\tau) = \frac{1}{\pi}\int_0^\infty J(\omega)\cos\left(\frac{r\omega}{v}\right)\frac{e^{\omega(\beta-|\tau|)} + e^{\omega|\tau|}}{e^{\beta\omega} - 1} d\omega, \quad (5)$$

whose nontrivial dependence on space and imaginary time is shown in Fig. 1(b). Notably, $K(r,\tau)$ can be written in a Lorentz-invariant form by introducing the complex coordinate $z = \tau + \frac{ir}{v}$. This reveals that the structure of the long-range interactions scales equivalently in the spatial- and imaginary-time directions, leading to the observed “collective decoherence" in contrast with the local criticality [27] and anomalous dynamical scaling [29] found in related models. The static limit of the bath interactions $K(r,\omega=0)=\int_0^\beta K(r,\tau)d\tau$ then defines the bosonic RKKY effect. Depending on the cutoff $f(\omega/\omega_c)$, the bosonic RKKY interactions are ferromagnetic,

$$K(r,\omega=0)=\frac{4\alpha\omega_c}{1+(Qr)^2},\quad \text{exponential cutoff,} \tag{6}$$

or oscillating,

$$K(r,\omega=0)=4\alpha\omega_c\frac{\sin(Qr)}{Qr},\quad \text{hard cutoff.} \tag{7}$$

These two distance dependencies are shown in Fig. 1(c). The characteristic momentum $Q\equiv\frac{\omega_c}{v}$ arises from the high-frequency cutoff and is analogous to $2k_F$ in the fermionic RKKY effect. In a BEC bath, this momentum can be identified with the inverse healing length $Q=\xi_h^{-1}$. Then, the spatial extent of the bath interactions is described by the dimensionless parameter $\lambda=(Qa)^{-1}=\xi_h/a$, where a is the lattice spacing. We focus on the exponential cutoff in Eq. (6) and leave the hard cutoff to future work [50].

Several limiting cases can be understood from the static interactions in Eq. (6). At high temperatures $k_BT\gg\Delta$, the DTFIM maps onto a classical $\frac{1}{r^2}$-Ising chain, which famously exhibits a BKT phase transition [51,52] to a long-range ordered ferromagnetic phase as α is increased [50]. At $T=0$, two limits lend themselves to analytical understanding: (i) The limit $\lambda\to\infty$ corresponds to the BEC healing length $\xi_h\gg a$ much longer than the lattice spacing, where all spins in the chain couple to each other equally and form one large "superspin" which behaves as the spin-boson model displaying a BKT transition [31,32]. In the opposite limit (ii) $\lambda\to 0$, the DTFIM maps onto a model where each spin couples to an independent bath [29,49]. In this work, we explore the most nontrivial case of finite $\lambda\sim 1$, and show that the resulting QCP has distinct critical exponents from the aforementioned limiting cases.

Methods. We study the DTFIM by performing classical Monte Carlo simulations on the 2D classical Ising model defined by the partition function in Eq. (2). In order to counteract the long autocorrelation times [53] due to frustrated interactions, the simulations were performed with a combination of Metropolis updates, modified Wolff cluster updates, and parallel tempering updates [49,54] (see Supplemental Material [48] and additional references therein [55–59]). The cluster updates are based on the long-range Wolff algorithm [60], however the mixed-sign interactions [see Fig. 1(b)] necessitate a modification where the acceptance probability for adding a given spin to the cluster is calculated from the absolute value of the interaction strength [48,49,61]. Parallel tempering [48,54,62] in the dissipation strength α is also employed, to aid in the convergence of the magnetization measurements and reduce the effects of critical slowing down. In the following, we study the total magnetization $m=[(NL)^{-1}\sum_{i,n}s(i,n)]$ that we use to compute the Binder cumulant

$$U_4=1-\frac{\langle m^4\rangle}{3\langle m^2\rangle^2} \tag{8}$$

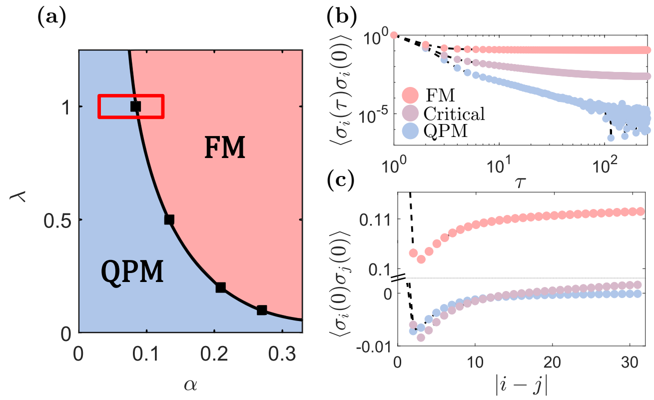

FIG. 2. The points shown (a) all belong to the second-order universality class described in this text. Extrapolating off the boundaries to $\lambda\to\infty$ and $\lambda\to 0$ results in BKT transitions. The disconnected correlation functions in the red-boxed region (a) are shown in (b) and (c), for values of $\alpha=\{0.035, 0.085, 0.09\}$, with power-law decay in τ and antiferromagnetic exponential decay in r in the QPM. Long-range ferromagnetic order dominates for $\alpha>\alpha_c$.

and the disconnected correlation function

$$C(|i-j|,\tau)=\langle\sigma_i(\tau)\sigma_j(0)\rangle \tag{9}$$

as probes of the critical properties and relevant phases. The angle brackets $\langle\cdot\rangle$ denote a Monte Carlo average.

Quantum critical point. The quantum paramagnet [QPM; the blue region in Fig. 2(a)] phase occurs for weak dissipation. As dissipation is increased beyond the critical value $\alpha_c(\lambda)$, the spins order ferromagnetically [FM; the red region in Fig. 2(a)]. The equal-time spatial correlations are all negative but their absolute value can otherwise be well described by an exponentially decaying function of the Ornstein-Zernike form [63] for 1 + 1D. The (positive/negative) parity of the correlations matches the form shown by the interactions along the $\tau=0$ axis in Fig. 1(b). The correlation length ξ is large, making the decay difficult to distinguish from a pure power law, but finite everywhere below the transition line $\alpha<\alpha_c(\lambda)$ in Fig. 2. At $\alpha=\alpha_c(L,\lambda)$ [Fig. 2(c)], the spatial correlations approach a finite value at the boundary. This is a finite-size effect which must be accounted for in the following analysis, but this finite value of $C(L/2,0)$ decays to 0 at $\alpha=\alpha_c(L,\lambda)$ in the limit $L\to\infty$ as expected at the QCP. For $\alpha>\alpha_c$, the correlations approach a positive (ferromagnetic) long-range limit [Fig. 2(c)], resulting in long-range order with $\langle m\rangle>0$. The local self-correlations in imaginary time $C(0,\tau)$ decay as a power law even deep in the QPM phase. This is consistent with the behavior in the single spin-boson model [8,29], which has algebraic correlations due to the power law in the interactions in Eq. (5).

The long-range interaction makes the finite-size corrections to the critical dissipation α_c significant, so great care is required in extracting the critical exponents [64]; see Supplemental Material [48]. In the following, we use the finite-size rounding of the transition in the limit of zero temperature to extract a strongly L-dependent crossover location $\alpha_c(L,\lambda)$, where in the following the argument λ will be suppressed. For fixed values of $L\in[8,192]$, we determine $\alpha_c(L)$ by

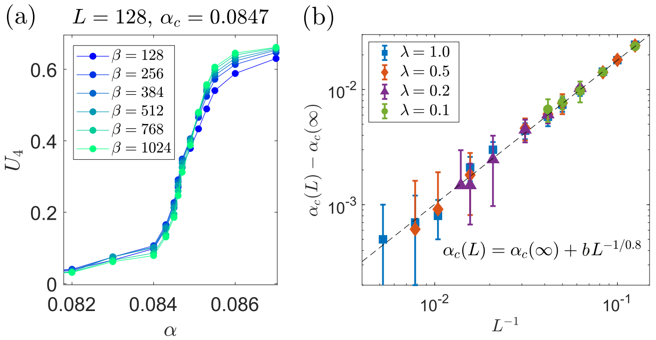

FIG. 3. (a) shows U_4 for fixed $\lambda = 1.0$, $L = 128$, with a series of β, giving $\alpha_c(L = 128) = 0.0847(5)$. For a given λ, ν and $\alpha_c(\infty, \lambda)$ are then found by fitting the values of $\alpha_c(L, \lambda)$ to the scaling relation $L^{-1} \sim [\alpha_c(L, \lambda) - \alpha_c(\infty, \lambda)]^{\nu}$, rearranged from Eq. (10). (b) shows the fits for multiple λ performed simultaneously, giving $\nu = 0.80(5)$.

extracting the points where $U_4(\alpha, \beta, L)$ lines cross, as shown in Fig. 3(a). The series of $\beta \in \{128, 256, 384, 512, 768, 1024\}$ is fixed, with N adjusted according to $\beta = N\tau_0$ and $\tau_0 = \omega_c^{-1}$. The finite value of τ_0 should not affect the universality [29].

From a series of $\alpha_c(L)$, the critical dissipation in the thermodynamic limit $\alpha_c(\infty)$ and the correlation length exponent ν can be determined by identifying L with the correlation length. The scaling law $\xi \sim (\alpha - \alpha_c)^{-\nu}$ implies the ansatz

$$\alpha_c(\infty) \sim \alpha_c(L) - bL^{-1/\nu} \tag{10}$$

for some constant b. Figure 3(b) shows a fit to this scaling ansatz for multiple values of the dimensionless bath extent λ. This demonstrates a collapse onto a universal scaling law relating $\alpha_c(L)$ and L with $\nu = 0.80(5)$, independent of λ. This indicates the entire phase boundary in Fig. 2(a) is governed by a common quantum critical universality class with the value of exponent ν that is distinct from both the case of Josephson junction arrays (limit $\lambda \to 0$) [29] and from the transverse field Ising model.

Finally, the correlation functions at the critical point can be used to determine the dynamical exponent z, and the anomalous dimension η. At the critical point, the connected same-time and same-site correlation functions for $D = 1 + z$ should follow the universal power-law relations [29]

$$\begin{aligned} C(r, \tau = 0) - \langle m \rangle^2 &\sim r^{-(z+\eta-1)}, \\ C(r = 0, \tau) - \langle m \rangle^2 &\sim \tau^{-(z+\eta-1)/z}, \end{aligned} \tag{11}$$

where $C(r, \tau)$ is defined in Eq. (9). These connected correlation functions are plotted in Figs. 4(a) and 4(b) [65,66], and the finite-size scaling in Figs. 4(c) and 4(d) allows us to extract the critical exponents $\eta = 1.02(6)$ and $z = 1.07(9)$.

Discussion. The DTFIM represents a clear example of long-range magnetic order induced by environmental bosonic interactions. By analogy to the fermionic RKKY effect, whose spatial dependence is governed by the UV momentum scale $2k_F$, a similar cutoff should appear in the bosonic RKKY effect. The analogous momentum scale is given by the inverse healing length $Q \sim \xi_h^{-1}$ or equivalently the UV cutoff $\omega_c = vQ$, which enters Eqs. (6) and (7). The oscillations implied by the term "RKKY" only appear in the case of a hard cutoff [Eq. (7)], which most closely resembles the sharp boundary of the Fermi level in fermionic systems. However, in the presently studied case of an exponential bath cutoff, the same mechanism produces the long-range ferromagnetic correlations. The value of the bath length scale $\lambda \sim Q^{-1}$ does not affect the universality of the QCP, but it does provide the length scale for the nontrivial short-range correlations exhibited by the QPM phase.

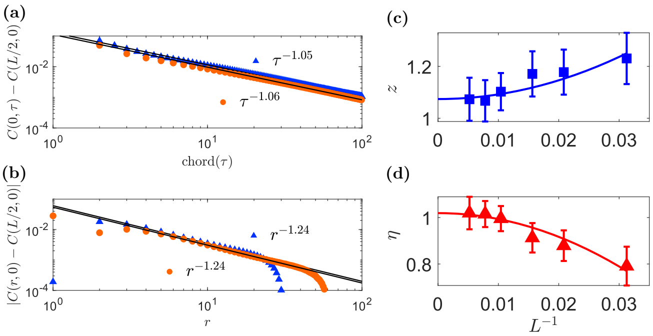

FIG. 4. Fits to the scaling form in Eq. (11) to determine η and z. The fits show power-law decay in the (a) same-site and (b) same-time correlation functions for $\lambda = 0.5$, $L = 64$, $\alpha_c = 0.1336$ (blue triangles) and $\lambda = 1.0$, $L = 128$, $\alpha_c = 0.084$ (orange circles), with $\mathrm{chord}(\tau) = \beta/\pi \sin(\pi\tau/\beta)$ (See Ref. [66]). (c) and (d) show $1/L$ extrapolations of z and η from the power-law fits for $\lambda = 1.0$ at the largest value of $\beta = 2048$. The $L \to \infty$ results are $z = 1.07(9)$ and $\eta = 1.02(6)$.

The critical exponents found here for finite λ characterize a different universality class, distinct from the previously studied limits of $\lambda \to \infty$ [31,32] and $\lambda \to 0$, which corresponds to each spin in a chain coupled to an independent bath [49]. In either of these two asymptotic cases, the quantum criticality reduces to a BKT transition of the single spin-boson model [7–9] that does not have two-dimensional Lorentz symmetry. With the inclusion of long-range bath-induced interactions, the Lorentz invariance of $K(r, \tau)$ in Eq. (5) that is broken by the transverse field Δ emerges at the QCP as we find $z = 1$, up to the uncertainty bounds in the present study. Physically, this is manifested by the collective decoherence found at the QCP, where the spins order spatially and in imaginary time simultaneously. Furthermore, the correlation length exponent takes an anomalous value $\nu = 0.80(5)$. By contrast to dissipative chains which include direct spin-spin interactions [29,46], the DTFIM provides an example of long-range magnetic order induced purely by a bosonic environment.

Experiments on ultracold mixtures in an optical lattice are an ideal setting to observe the phases and to explore the QCP we have identified. The phases and critical properties can be ascertained by measuring correlation functions using single-site-resolved quantum gas microscopy [67] or through optical Bragg scattering [68]. The presence of a harmonic trap will produce an additional length scale that will round out the critical properties that we predict. Nonetheless, varying the strength of potential should allow one to see the universal scaling properties before being rounded out, but this issue can be circumvented using a box trap [69]. This study was limited to the Ohmic spectral density due to the assumption of the form of spin-bath couplings g_k relevant to BEC bath [26], but an exploration of sub- and super-Ohmic baths could also prove interesting for future studies.

Acknowledgments. M.W.B. and A.H.N. were supported by the Robert A. Welch Foundation Grant No. C-1818. A.H.N. was also supported by the National Science Foundation Division of Materials Research Award No. DMR-1917511. J.H.P. is partially supported by NSF CAREER Grant No. DMR-1941569, by the Air Force Office of Scientific Research under Grant No. FA9550-20-1-0136, and the Alfred P. Sloan Foundation through a Sloan Research Fellowship. The Flatiron Institute is a division of the Simons Foundation. All calculations were performed on the Rice University's Center for Research Computing (CRC), supported in part by the Big-Data Private-Cloud Research Cyberinfrastructure MRI-award funded by NSF under Grant No. CNS-1338099. M.W.B. and A.H.N. acknowledge the hospitality of the Kavli Institute for Theoretical Physics (supported by the NSF Grant No. PHY-1748958), where a portion of this work was performed.

[1] I. L. Chuang, R. Laflamme, P. W. Shor, and W. H. Zurek, Science **270**, 1633 (1995).
[2] J. H. Reina, L. Quiroga, and N. F. Johnson, Phys. Rev. A **65**, 032326 (2002).
[3] P. W. Shor, Phys. Rev. A **52**, R2493 (1995).
[4] A. Steane, Rep. Prog. Phys. **61**, 117 (1998).
[5] W. G. Unruh, Phys. Rev. A **51**, 992 (1995).
[6] W. H. Zurek, Phys. Today **44**(10), 36 (1991).
[7] A. J. Bray and M. A. Moore, Phys. Rev. Lett. **49**, 1545 (1982).
[8] S. Chakravarty, Phys. Rev. Lett. **49**, 681 (1982).
[9] A. O. Caldeira and A. J. Leggett, Ann. Phys. **149**, 374 (1983).
[10] A. J. Leggett, S. Chakravarty, A. T. Dorsey, M. P. Fisher, A. Garg, and W. Zwerger, Rev. Mod. Phys. **59**, 1 (1987).
[11] W. H. Zurek, Phys. Rev. D **24**, 1516 (1981).
[12] W. H. Zurek, Phys. Rev. D **26**, 1862 (1982).
[13] I. Bloch, J. Dalibard, and W. Zwerger, Rev. Mod. Phys. **80**, 885 (2008).
[14] A. Rubio-Abadal, J.-y. Choi, J. Zeiher, S. Hollerith, J. Rui, I. Bloch, and C. Gross, Phys. Rev. X **9**, 041014 (2019).
[15] C. Sabín, A. White, L. Hackermuller, and I. Fuentes, Sci. Rep. **4**, 6436 (2015).
[16] F. Schäfer, N. Mizukami, P. Yu, S. Koibuchi, A. Bouscal, and Y. Takahashi, Phys. Rev. A **98**, 051602(R) (2018).
[17] M. A. Ruderman and C. Kittel, Phys. Rev. **96**, 99 (1954).
[18] T. Kasuya, Prog. Theor. Phys. **16**, 45 (1956).
[19] K. Yosida, Phys. Rev. **106**, 893 (1957).
[20] J. I. Cirac and P. Zoller, Phys. Rev. Lett. **74**, 4091 (1995).
[21] M. Mirhosseini, A. Sipahigil, M. Kalaee, and O. Painter, Nature (London) **588**, 599 (2020).
[22] A. Bienfait, K. J. Satzinger, Y. P. Zhong, H.-S. Chang, M.-H. Chou, C. R. Conner, E. Dumur, J. Grebel, G. A. Peairs, R. G. Povey, and A. N. Cleland, Science **364**, 368 (2019).
[23] B. J. DeSalvo, K. Patel, G. Cai, and C. Chin, Nature (London) **568**, 61 (2019).
[24] R. Bouganne, M. Bosch Aguilera, A. Ghermaoui, J. Beugnon, and F. Gerbier, Nat. Phys. **16**, 21 (2020).
[25] V. Kasper, D. González-Cuadra, A. Hegde, A. Xia, A. Dauphin, F. Huber, E. Tiemann, M. Lewenstein, F. Jendrzejewski, and P. Hauke, Quantum Sci. Technol. **7**, 015008 (2022).
[26] P. P. Orth, I. Stanic, and K. Le Hur, Phys. Rev. A **77**, 051601(R) (2008).
[27] S. Tewari, J. Toner, and S. Chakravarty, Phys. Rev. B **72**, 060505(R) (2005).
[28] S. Tewari, J. Toner, and S. Chakravarty, Phys. Rev. B **73**, 064503 (2006).
[29] P. Werner, K. Volker, M. Troyer, and S. Chakravarty, Phys. Rev. Lett. **94**, 047201 (2005).
[30] D. Patanè, A. Silva, L. Amico, R. Fazio, and G. E. Santoro, Phys. Rev. Lett. **101**, 175701 (2008).
[31] A. Winter and H. Rieger, Phys. Rev. B **90**, 224401 (2014).
[32] G. De Filippis, A. de Candia, A. S. Mishchenko, L. M. Cangemi, A. Nocera, P. A. Mishchenko, M. Sassetti, R. Fazio, N. Nagaosa, and V. Cataudella, Phys. Rev. B **104**, L060410 (2021).
[33] Y.-Z. Wang, S. He, L. Duan, and Q.-H. Chen, Phys. Rev. B **103**, 205106 (2021).
[34] N. Zhou, Y. Zhang, Z. Lü, and Y. Zhao, Ann. Phys. **530**, 1800120 (2018).
[35] T. A. Costi and R. H. McKenzie, Phys. Rev. A **68**, 034301 (2003).
[36] D. P. S. McCutcheon, A. Nazir, S. Bose, and A. J. Fisher, Phys. Rev. B **81**, 235321 (2010).
[37] T. Zell, F. Queisser, and R. Klesse, Phys. Rev. Lett. **102**, 160501 (2009).
[38] P. P. Orth, D. Roosen, W. Hofstetter, and K. Le Hur, Phys. Rev. B **82**, 144423 (2010).
[39] M. Cattaneo, G. L. Giorgi, S. Maniscalco, and R. Zambrini, New J. Phys. **21**, 113045 (2019).
[40] G. Karpat, I. Yalcinkaya, and B. Cakmak, Phys. Rev. A **101**, 042121 (2020).
[41] A. Strathearn, P. Kirton, D. Kilda, J. Keeling, and B. W. Lovett, Nat. Commun. **9**, 3322 (2018).
[42] K. Seetharam, A. Lerose, R. Fazio, and J. Marino, Phys. Rev. Research **4**, 013089 (2022).
[43] J. Marino and S. Diehl, Phys. Rev. B **94**, 085150 (2016).
[44] J. H. Pixley, L. Deng, K. Ingersent, and Q. Si, Phys. Rev. B **91**, 201109(R) (2015).
[45] A. M. Lobos, M. A. Cazalilla, and P. Chudzinski, Phys. Rev. B **86**, 035455 (2012).
[46] I. B. Sperstad, E. B. Stiansen, and A. Sudbo, Phys. Rev. B **81**, 104302 (2010).
[47] S. Sachdev, *Quantum Phase Transitions*, 2nd ed. (Cambridge University Press, Cambridge, UK, 2011).
[48] See Supplemental Material at http://link.aps.org/supplemental/10.1103/PhysRevB.105.L180407 for technical details of the quantum-to-classical mapping, the Monte Carlo cluster update algorithm, and additional data at different system sizes and values of the imaginary-time spacing τ_0.
[49] M. W. Butcher, J. H. Pixley, and A. H. Nevidomskyy, AIP Adv. **8**, 101415 (2018).
[50] M. W. Butcher, J. H. Pixley, and A. H. Nevidomskyy (unpublished).
[51] D. J. Thouless, Phys. Rev. **187**, 732 (1969).
[52] E. Luijten and H. Messingfeld, Phys. Rev. Lett. **86**, 5305 (2001).

[53] M. Troyer and U.-J. Wiese, Phys. Rev. Lett. **94**, 170201 (2005).
[54] E. Marinari and G. Parisi, Europhys. Lett. **19**, 451 (1992).
[55] K. Hukushima and K. Nemoto, J. Phys. Soc. Jpn. **65**, 1604 (1996).
[56] M. Hasenbusch, J. Stat. Mech. (2008) P08003.
[57] E. Granato, Phys. Rev. B **85**, 054508 (2012).
[58] R. H. Swendsen and J.-S. Wang, Phys. Rev. Lett. **57**, 2607 (1986).
[59] U. Wolff, Phys. Rev. Lett. **62**, 361 (1989).
[60] E. Luijten and H. W. Blöte, Int. J. Mod. Phys. C **06**, 359 (1995).
[61] M. Pleimling and M. Henkel, Phys. Rev. Lett. **87**, 125702 (2001).
[62] D. J. Earl and M. W. Deem, Phys. Chem. Chem. Phys. **7**, 3910 (2005).
[63] M. Campanino, D. Ioffe, and Y. van Velenik, Probab. Theory Relat. Fields **125**, 305 (2003).
[64] Normally, the location of the critical point, as well as the correlation length and dynamical exponent z, can be determined by the collapse of the Binder cumulant $U_4(\alpha_c, \lambda, \beta, L) = U_4(\alpha_c, \lambda, \beta/L^z)$ as in Refs. [29,46]. Unfortunately, finite-size corrections leads to this procedure failing for this model.
[65] In order to plot the connected correlation function, we subtract the magnetization squared $\langle m\rangle^2$, which we extract from the value of $C(r = L/2, 0)$ on a finite-size system, relying on the identity $\lim_{r\to\infty} C(r, 0) = \langle m\rangle^2$.
[66] The chord function is a consequence of the conformal mapping [47] for finite-T correlators $v\tau \pm ir \to \frac{\beta v}{\pi}\sin[\frac{\pi}{\beta v}(v\tau \pm ir)]$. Although we are studying the results for $T = 0$, the finite size of our system requires the use of finite β here. Since $\beta v \gg r$, the approximation $\sinh(r) \sim r$ is used in the case of the spatial correlations.
[67] A. Mazurenko, C. S. Chiu, G. Ji, M. F. Parsons, M. Kanász-Nagy, R. Schmidt, F. Grusdt, E. Demler, D. Greif, and M. Greiner, Nature (London) **545**, 462 (2017).
[68] T. A. Corcovilos, S. K. Baur, J. M. Hitchcock, E. J. Mueller, and R. G. Hulet, Phys. Rev. A **81**, 013415 (2010).
[69] A. L. Gaunt, T. F. Schmidutz, I. Gotlibovych, R. P. Smith, and Z. Hadzibabic, Phys. Rev. Lett. **110**, 200406 (2013).